Physicochemical and toxicological evaluation of silica nanoparticles suitable for food and consumer products collected by following the EC recommendation

Catia Contado [1,*]

Email catia.contado@unife.it

Jorge Humberto Mejia Mendoza [2]

Omar Lozano García [2]

Jean-Pascal Piret [3]

Elise Dumortier [3]

Olivier Toussaint [3]

Stéphane Lucas [2]

[1] Department of Chemical and Pharmaceutical Sciences, University of Ferrara, via L. Borsari, 46, 44121 Ferrara, Italy

AQ2

[2] Research Centre for the Physics of Matter and Radiation (PMR-LARN), Namur Nanosafety Center (NNC), NAmur Research Institute for LIfe Science (NARILIS), University of Namur, Rue de Bruxelles 61, 5000 Namur, Belgium

[3] Research Unit in Cellular Biology (URBC), NNC-NARILIS, University of Namur, Rue de Bruxelles 61, 5000 Namur, Belgium

Abstract

Specific information about the particle size distribution, agglomeration state, morphology, and chemical composition of four silica samples, used as additives in food and in personal care products, were achieved with a combination of analytical techniques. The combined use of differential centrifugal sedimentation (DCS), sedimentation field flow fractionation (SdFFF), and scanning and transmission electron microscopy (SEM and TEM) allows to classify the water dispersed samples as “nanomaterials” according to the EC definition. The mechanical stirring and the ultrasound treatment were compared as dispersion methods. The particle surface chemical composition, ~~was~~ determined by particle-induced X-ray emission (PIXE) and X-ray photoelectron spectroscopy (XPS), assessed the different levels of purity

between the pyrogenic and the precipitated silica and highlighted particle surface chemical composition modifications in the outer shell when dispersed by mechanical stirring. The potential toxic effects of silica on intestinal Caco-2 cells were investigated using MTS assay and by measuring lactate dehydrogenase (LDH) release and caspases 3/7 activity after 24 h of incubation. No or limited decrease of cell viability was observed for all particles regardless of dispersion procedure, suggesting a relative innocuity of these silica samples.

Keywords

Silica nanoparticles
Food additives
Surface analysis
In vitro tests
Differential centrifugal sedimentation (DCS)
Sedimentation field flow fractionation (SdFFF)

Published in the topical collection *Field- and Flow-based Separations* with guest editors Gaetane Lespes, Catia Contado, and Bruce Gale.

Electronic supplementary material

The online version of this article (doi: 10.1007/s00216-015-9101-8) contains supplementary material, which is available to authorized users.

Introduction

Amorphous silicon dioxide (SiO_2 or silica) is industrially produced through several methods, each of which imparts different chemical and physical characteristics to SiO_2; these differences make them suitable for a variety of commercial applications [1].

In the food industry, amorphous silica (SiO_2) is registered and approved as food additive (coded E551). SiO_2 has no nutritional value, but it is one of the most used materials, together with titanium dioxide and magnesium oxide, to preserve color or durability, to improve handling, and to carry fragrances or flavors. SiO_2 is also used as anti-caking agent to maintain flow properties of powdered mixes, seasonings, and coffee whiteners. The improvement of the production efficiency and product characteristics, brought by the nanotechnologies in the food and feed industries [2], has meant for the silica particles their reduction to the nanoscale [3, 4].

The present EU legislation requires that in the list of ingredients for food, cosmetics, and biocide products, the “nanomaterials”, if present, be reported with “nano” added in brackets after the substance name [5, 6]. This precautionary and general regulation comes from the awareness that many types of nanoparticles (NPs) are potentially toxic on isolated cells [7] and that to improve knowledge of their real effects on humans and

environment requires time. In the meanwhile, consumers are empowered to decide if they want to buy a product that contains NPs.

The biological effects caused by the NPs are related, in addition to concentration and exposure time, to their physicochemical properties such as size, shape, surface charge, hydrophobicity, etc.; consequently, information about these parameters should adequately complement the toxicological assays. Unfortunately, some of these parameters, such as mass, total surface area, and number of particles, or a combination of these parameters (e.g., NP mass/surface unit –NPs μg/cm^2) [8, 9], are not always unequivocally well definable since they change depending on the pH, ionic strength, and physiological media composition.

The European Food Safety Authority (EFSA) [10] advices to characterize the NPs suitable for food applications at five distinct stages: as manufactured, as delivered for use in food/feed products, as present in the food/feed matrix, as used in toxicity testing, and as present in biological fluids and tissues. The same NP physicochemical characteristic (e.g., aggregation state), determined in each stage, could bring to very different results but what matters is not as much the consistency of the data but rather the information itself, which might be relevant for specific exposure situations; for example, NPs characterized “as manufactured” concern the workers exposure, in the food/feed matrix, they are relevant for the interaction testing and in the biological fluids and tissues, they matter for the “absorption, distribution, metabolism, and excretion” (ADME) studies.

In this study, two pyrogenic synthetic amorphous silica and two precipitated synthetic amorphous silica were examined as manufactured (I° stage). The silica were dispersed in deionized water, with the aims of determining, firstly, whether they meet the EC definition of “nanomaterials,” secondly, if the dispersion procedures affect the particle size distributions and/or the chemical surface composition, and thirdly, if these silica particles cause toxic effects on human intestinal Caco-2 cells.

AQ3

To accomplish the first task according to the EC recommendation [11], the sedimentation field flow fractionation (SdFFF) [12] and the differential centrifugal sedimentation (DCS) [13] techniques were used in combination to determine the particle size distributions (PSDs). Both techniques sort the samples in their component by the action of the centrifugal field, but the SdFFF, as an elution chromatographic-like technique, allows to recover the separated components for further characterization [12]. This very simple matrix allows to equip the SdFFF with an UV-vis detector, reducing the analysis costs. The SdFFF and DCS results were elaborated in order to produce PSDs expressed in terms of particle weight and particle number-related distributions, as required by the EC definition [11], with the awareness that the UV-signal scattered by the particles depends on the particle sizes [14]. ~~Transmission electron microscope (TEM) and s~~Scanning electron microscope (SEM) observations were done to gain

information about the particle shape, the morphology, and the aggregation state.

Some recent publications in the field of food NP characterization sponsor and support the use of separation techniques coupled with element-specific detectors, such as ICP-MS, ICP-AES, and/or AAS. This is absolutely advisable and recommended, but it is also a good practice to proportion the analysis costs and the time required for them for the purpose of the study. The purpose of this paper is to draw the attention to some experimental steps, often underestimated, which, in turn, might be important during the NP characterization and not to present an analytical method suitable to determine the silica NPs inside commercial products.

The information about the size and the shape of the particles were enriched with the surface and the bulk elemental composition data determined by X-ray photoelectron spectroscopy (XPS) and the particle-induced X-ray emission (PIXE). PIXE is a very powerful technique able to identify and quantify elements also in complex matrices [15], but here, together with the XPS, it has been used mainly to determine the chemical composition of the bulk and the outer surface layer of the SiO_2 particles before and after their dispersion in deionized water applying two different procedures: an ultrasound treatment (US) and a vigorous magnetic stirring (MS). This aspect, investigated in the case of MWCNTs [16] and SiC and TiC [17] particles, has never been considered before for SiO_2 samples. The XPS and PIXE analyses were done also on the SiO_2 water dispersions, coarsely divided in fractions, enriched with particles of selected sizes (nominally <40 or 300 nm, depending on the silica type).

The potential cytotoxicity effects of the SiO_2 particles were evaluated on Caco-2 cells, chosen as a model for human intestinal epithelial cells. These particles could be actually inhaled during their manufacture, but the work and health safety and the consolidated scientific knowledge of the biological effects connected with the inhalation, as possible route of exposure, move this aspect to the background respect to the possible ingestion when these silica are added to food, pharmaceutical, and personal care products.

To our best knowledge, only few studies are available [7, 18–23] on this subject and none of them considers the possible effects introduced by the dispersion methods.

To conclude, two examples of very simple food products, a powdered “Cappuccino mix,” claiming the E551 content and an instant barley silica-free coffee were analyzed by PIXE and DCS to detect presence of silica NPs and evaluate their particle size distribution. The food products were prepared as indicated on their labels for a homemade preparation.

Experimental

Materials

Pyrogenic synthetic amorphous silica of high purity Aerosil300® (A300) and

Aerosil380® (A380) (Evonik-Degussa) were kindly donated by EigenMann & Veronelli SpA. The physical specifications given by the manufacturers are an average primary particle size of 7 nm and a BET surface area of 300 and 380 m^2/g respectively, confirmed by a series of publications [24, 25].

Precipitated synthetic amorphous silica Tixosil43 (T43) and Tixosil73 (T73) (Rhodia) were a kind gift from Biophyl Italia SpA. The declared average particle diameters are 8–10 μm [26, 27].

Deionized water from a Milli-Q system (Millipore-Merk, Vimodrone, Milan, Italy) was used all through the experiments. All other solvents and chemicals were of the highest grade commercially available, usually purchased from Backer.

Instant barley coffee (silica free) and instant cappuccino mix (containing E551) powders were purchased in an Italian local grocery.

Instruments

Sedimentation field flow fractionation

The sedimentation field flow fractionation (SdFFF) system was a Model S101 Colloid/Particle Fractionator (Postnova Analytics, Landsberg, Germany) well described elsewhere [28]. An HPLC pump PN1121 (Postnova Analytics) usually pumped the mobile phase at 2.0 mL/min. Sample suspensions were injected through a 50-μL Rheodyne loop valve. The particle elution was monitored by a UV/Vis detector Spectra SERIES UV100 (Thermo Separation Products, USA) operating at a fixed wavelength of 254 nm. The SPIN 1409 program, used to acquire the fractrograms, controlled the SdFFF instrument; the FFF ANALYSIS program processed the acquired data; both were Windows compatible programs provided by Postnova Analytics together with the instrument. The fractionations were performed using a power programming mode [29] to reduce the time necessary for analysis (see Table S1 for the field parameters).

Differential centrifugal sedimentation

The DC24000 system (CPS instruments Inc., Stuart, Florida, USA) was equipped with a 405-nm wavelength laser detector. For each differential centrifugal sedimentation (DCS) analysis, 0.3 mL of sample suspensions was injected into a stepwise density sucrose gradient of 2–8 % *w*/*w*, and 2.2 and 2.1 g/mL were the densities used respectively for the Aerosil and Tixosil samples. The sizes are expressed in terms of hydrodynamic diameter assuming all particles were spherical. The accuracy of measured sizes is ensured before each test by a certified PVC standard (particle size, 0.226 μm) [13]. The PSD of the analyzed suspensions are given as weight and number-related distributions. Two measurement protocols were established, one for the Aerosil samples and one for the Tixosil ones, differing mainly on the lower size limit. Each protocol measures a different range of sizes: from 3 nm to 20 μm (22,000 rpm) and from 20 nm to 20 μm (13,000 rpm) for Aerosil and Tixosil samples, respectively. A refractive index of 1.46

was used for both silicas, while a value of 1.34 was set for the solvent.

All suspensions were mixed with a vortex for 1 min prior to being analyzed.

Particle-induced X-ray emission

The element concentration on commercial samples and on silica fractions was measured by particle-induced X-ray emission (PIXE) on the ALTAÏS accelerator of the University of Namur. The incident ion beam was 2.5 MeV protons. The geometry and setup for the measurements is described elsewhere [30]. Briefly, with respect to the beam direction, the sample was tilted at 45°, and a Canberra LEGe (low energy germanium) detector was located at 90° for PIXE measurements. An aluminum collimator (1 mm aperture, 0.2 mm thick) was used in front of the PIXE detector. PIXE measurements were validated with two standards from the International Atomic Energy Agency (IAEA 153 and IAEA 155). The results are in agreement with respect to the reported concentrations (better than 5 %) [31, 32]. Limits of detection (LOD) were extrapolated for each element (based on the generated background noise) and was estimated at 0.435 μg/mL for Si [33].

X-ray photoelectron spectroscopy

X-ray photoelectron spectroscopy (XPS) spectra of silica samples and the derived fractions were recorded with a K-alpha (THERMO Scientific) equipped with a hemispherical electron analyzer using mono-chromatized Al Kα radiation as excitation source (1486.6 eV). All reported spectra were recorded at 90° take-off angle. The XPS analysis depth is around 5 nm. Core-level lines (C1s, Si2p) were calibrated to the C1s peak (284.6 eV). The spectra were analyzed, fitting the Gaussian function to the experimental curve, with a non-linear least squares scheme, and using a Shirley background. Nominal resolution was measured as full width at half maximum of 1.0 eV (core-level spectrum) to 1.5 eV (survey spectrum).

Other apparatus

A ~~transmission electron microscope (TEM) (Hitachi H-800) and a~~ ZEISS EVO 40 scanning electron microscope (SEM) ~~were~~was used to evaluate both size and morphology of the particles. The samples for the ~~T~~SEM observations were prepared by ~~depositing~~filtering ~~a drop of aqueous suspension on a copper grid (mesh 150) and let dry in an oven at 40 °C prior to its use. For the SEM observations,~~ 1 mL of a diluted suspension ~~was filtered~~ on Isopore™ membranes (0.1-μm pore size), then glued onto aluminum stubs using double-adhesive tape (TAAB Laboratories Equipment, Ltd. Aldermaston, Berkshire, UK).

Methods

Silica suspensions preparations—A300, A380, T43, T73 samples

The 2 mg/mL suspensions were prepared by dispersing the silica particles (A300, A380

and T43, T73) in deionized water. The four suspensions were mixed on a vortex for 30 s and then (1) stirred using a magnetic bar for 15 min at 400 rpm (method A), (2) sonicated with a 2-mm wide US probe for 120 s−50 % power (10 W) (method B); and (3) placed in an US sonicator water bath (180 W−50 Hz) for 15 min (method C) (see also Table S2).

For the cell viability tests, the four silica suspensions were prepared following the methods A and C and by lowering the concentration to 1 mg/mL.

A380 and T43 silica fractions preparation

Fractions of sonicated and stirred A380 and T43 silica were obtained by stirring (method A described above) or by sonication with a 2-mm wide probe for 120 s−50 % power (10 W) (method B) approximately 10 mg/mL of the A380 and T43 powders. These four suspensions were centrifuged at 13,000 rpm (Minispin Eppendorf centrifuge with rotor F-45-12-11) for 50 min (A380) and 2 min (T43) to collect supernatant suspensions, containing respectively particles nominally <40 nm (A380) and 300 nm (T43). Their volume was reduced at ~2 mL, evaporating the water at 70 °C (see Fig. S2). The sediments were dispersed in roughly 10 mL of deionized water. The estimated concentrations determined by DCS are reported in Table S3.

Particle digestion in gastric juice

The A380 and T43 powder samples and their dried sediment fractions, achieved from methods A and B, were incubated in simulated gastric fluid as the following: a weighted amount of sample was placed in contact with 5 mL of a simulated gastric fluid solution (50 mL HCl 0.1 N + 0.32 % *w*/*v* Pepsin (160 mg) + 0.2 % *w*/*v* NaCl (100 mg)). The suspensions were incubated for 4 h, after which the pH was increased from 1–2 up to ~7 by adding NaOH 0.1 N. Table S4 collects all the numerical information about this procedure.

Specimen preparation for the XPS analyses

A fraction of the A300, A380 and T43, and T73 silica powders were placed and pressed on a double face carbon tape. To analyze the silica dispersed in water (wet form), one drop of each suspension was let dry at room temperature (about 24 h) on a gold slab and stored in a plastic box to avoid contamination. The detection limit of the method is about 0.1 % of the atoms (at.%). Data are presented in Tables 1 and 3.

Table 1

Surface particle chemical composition determined by XPS. Analyses performed on the original silica powders, as commercially available

AQ4

Sample	A300	A380	T43	T73
at.% atomic %				

Sample	A300	A380	T43	T73
at.% Si	37.3 ± 3.1	36.7 ± 3.3	35.2 ± 0.3	36.5 ± 0.8
at.% O	60.6 ± 2.9	58.0 ± 3.1	59.7 ± 1.4	60.5 ± 0.2
O:Si ratio	1.6	1.6	1.7	1.7
at.% C	2.2 ± 0.7	1.58 ± 0.3	4.7 ± 1.6	3.0 ± 1.0
at.% atomic %				

Specimen preparation for the PIXE analyses

The sample holder has a truncated conical shape (2 cm in diameter, 4 mm of depth, and 2 mm in the truncation), in order to hold a droplet for drying and preventing horizontal spread. The specimens were prepared from stock dispersions by depositing a total volume of 200 μL, subdivided in 10 aliquots of 20 μL each (drying droplet methodology to avoid sample loss in the air [30]). Between each deposition, the droplet was dried in an oven for 1 h at 60 °C. Before taking each droplet, the suspensions were vortexed for 5 s. Double-face carbon tape was placed on top of the holder, providing a conductive surface and almost no background noise for the PIXE measurements. The sample T73 was deposed on the support for the PIXE analysis as powder. Table 2 reports the PIXE results on the silica samples, while Table ~~3~~4 reports the results for the A380 and T43 and all the fractions derived from them. For the fractions, the contribution due to the dissolved salts in the deionized water was accounted by preparing a "blank solution," evaporating 150 mL of water at 70 °C, with the same concentration ratio used for the supernatant fractions.

Table 2

Particle chemical composition determined by PIXE

	Si		P		S		Ti		K		Ca	
	ppm	%[c]	ppm	%[c]	ppm	%[c]	ppm	%[c]	ppm	%[c]	ppm	
A300[a]	475000 ± 1045	46.5 ± 0.1	5283 ± 835	0.52 ± 0.08					86 ± 41	0.008 ± 0.004	134 ± 24	0 ± 0
A380[a]	475000 ± 3895	46.4 ± 0.2	3678 ± 553	0.36 ± 0.05					449 ± 91	0.04 ± 0.01		
T43[a]	475000 ± 1853	46.3 ± 0.2	2769 ± 564	0.27 ± 0.06	2864 ± 265	0.28 ± 0.03					2649 ± 112	0 ± 0
[a]Samples analyzed as dispersions (suspension prepared according the method A and deposed 10												
[b]Samples analyzed as powder (sample measured as a pellet)												
[c]Mass percentage calculation include estimated oxygen content from silica formulation (SiO_2): 2 silicon atom												

	Si		P		S		Ti		K		Ca	
	ppm	%[c]	ppm	%[c]	ppm	%[c]	ppm	%[c]	ppm	%[c]	ppm	
T73[b]	420000 ± 1008	46.5 ± 0.1	2418 ± 382	0.28 ± 0.04	1041 ± 124	0.12 ± 0.01	340 ± 37	0.04 ± 0.004			193 ± 34	0 ± 0

[a]Samples analyzed as dispersions (suspension prepared according the method A and deposed 10 t

[b]Samples analyzed as powder (sample measured as a pellet)

[c]Mass percentage calculation include estimated oxygen content from silica formulation (SiO_2): 2 silicon atom

Table 3

Particle surface chemical composition from XPS measurements done on the fractionated samples A380 and T43, dispersed according the methods A and B

	Method A (stirred)		Method B (probe sonication)	
Sample A380	Supernatant	Sediment	Supernatant	Sediment
at.% Si	28.8 ± 1.4	32.2 ± 6.3	33.4 ± 0.4	34.4 ± 4.4
at.% O	44.3 ± 1.9	18.1 ± 0.5	56.7 ± 0.8	19.1 ± 4.0
O:Si ratio	1.5	0.56	1.7	0.55
at.% C	24.2 ± 2.4	45.6 ± 4.6	5.5 ± 0.4	41.1 ± 4.1
at.% Na	2.7 ± 0.8	4.1 ± 2.0	3.1 ± 0.2	
Sample T43	Supernatant	Sediment[a]	Supernatant	Sediment
at.% Si	6.0 ± 2.8	4.9 ± 2.5	27.3 ± 0.9	35.0 ± 1.1
at.% O	43.1 ± 0.2	59.0 ± 23.1	51.8 ± 1.1	58.7 ± 2.3
O:Si ratio	6.8	12.04	2.5	1.7
at.% C	29.2 ± 5.4	17.8 ± 2.6	11.2 ± 1.7	5.1 ± 2.5
at.% Na	13.6 ± 1.6	–	10.3 ± 3.4	0.7 ± 0.1

[a]at.% Ca = 6.5 ± 3.4

Cell culture

Human colon carcinoma Caco-2 cells were purchased from European Collection of Cell Cultures (ECACC). Caco-2 cells were maintained in culture in 75-cm^2 polystyrene flasks (Costar) with Dulbecco's modified Eagle's medium high glucose (DHG) solution (Gibco) containing 1 % ~~(~~*v*/*v*~~)~~ non-essential amino acids (Gibco) and 10 % fetal bovine serum (Gibco). This medium was supplemented with antibiotics (penicillin/streptomycin, Gibco). Cells were grown at 37 °C in a 5 % CO_2 incubator with humidified air.

MTS assay

The CellTiter 96® AQueous One Solution Cell Proliferation Assay (Promega) is a colorimetric method for determining the number of viable cells in proliferation.

The reduction of MTS tetrazolium salt (3-(4,5-dimethyl-thiazol-2-yl)-5-(3-carboxy-methoxyphenyl)-2-(4-sulfophenyl)-2H-tetrazolium) by metabolically active cells into its reduced formazan form was assessed following manufacturer's instructions. Non-viable cells do not reduce MTS tetrazolium salt, whereas a lower amount of colored reduced formazan is measured in the absence of cell proliferation.

Briefly, 20,000 Caco-2 cells/well were seeded in 500 µL of complete culture media in 24-well plates (Corning). After 24 h of incubation in the presence or not (control CTL) of silica (100 µg/mL), culture medium was collected for interleukine-8 measurements (by ELISA; see Supplementary Material) and measurement of released lactate dehydrogenase (LDH; see below). Cells were then washed once with fresh culture medium and incubated at 37 °C for 3 h in the presence of MTS substrate before measuring the absorbance at 490 nm with a spectrophotometer (xMark, Biorad).

Benzalkonium chloride (BC; 0.01 mg/mL, Sigma) was used as positive control for cell death.

To take into account the potential interference of silica with the MTS assay, optical density (OD) values corresponding to culture medium incubated with NPs (no cell) were used as respective assay blanks and subtracted to corresponding conditions. Results are expressed as percentages of controls.

LDH colorimetric assay

Released LDH in cell culture medium was assessed with the "Cytotoxicity Detection kit" (Roche) according to manual instructions. In case of cytotoxicity/cytolysis, intracellular LDH is released from damaged cells into culture medium where its activity can be measured using a specific substrate. Twenty-four hours after NP incubation (100 µg/mL), cell culture media were collected and centrifugated at 13,000 rpm for 5 min. One hundred microliters of supernatants were mixed with 100 µL of LDH substrate and incubated at room temperature for 30 min before measuring 490 nm absorbance (reference wavelengths of 655 nm) with a spectrophotometer (xMark, Biorad). OD values were normalized with cellular protein content. Protein concentrations were assayed on cell lysates (obtained by incubation of 30 min with M-Per buffer—Thermo Scientific—60 µL/well) with the "Pierce 660 nm Protein Assay Reagent" (Thermo Scientific). Results were normalized to controls.

BC (0.01 mg/mL, Sigma) was used as positive control for cell death.

Caspases 3/7 activity assay

Potential pro-apoptotic effect of silica NPs was evaluated using the Apo-ONE®

Homogeneous Caspase-3/7 Assay (Promega). In order to respect the same cell density used with MTS and LDH assays (24-well plate), Caco-2 cells were seeded at 3500 cells/well in a black 96-well plate (Greiner) and incubated for 24 h with 85 μL of culture medium containing NPs at 100 μg/mL. This volume ensured the respect of the same NP dose/surface unit between 96- and 24-well plate (26.56 μg/cm^2). Cells were then incubated for 3 h at room temperature with an equivalent volume of profluorescent caspases 3/7 substrate rhodamine 110 (Z-DEVD-R110) diluted in lysis buffer. Cleavage of the non-fluorescent substrate by caspases led to the release of fluorescent R110 measured with a Fluoroskan Ascent (Thermo Electron Corporation) (excitation wavelength, 485 nm; emission wavelength, 538 nm).

Butyrate (50 mM, Sigma) was used as positive control [34].

Statistical analysis

Data were obtained at least in triplicate averaged. Results are expressed as mean ± standard deviation (SD). Analysis of statistical significance was done using Student's *t* tests with $*P < 0.05$ as level of significance.

Commercial samples

Roughly 0.1 g of barley coffee powder and 1.5 g of "Cappuccino mix" powder were dissolved in 10 mL of hot deionized water (100 °C). These proportions assure a final concentration that mimic a typical homemade preparation, i.e., the concentration suggested on the product label by dissolving "a teaspoon of powder in a cup—240 mL—of hot water." The suspensions were stirred at 90 °C for 5 min and then let cool at room temperature. The resulting suspensions were analyzed by DCS, while PIXE analyses were done on the powders.

Results and discussion

The physicochemical characterization done in this study is aimed to provide a clear information about the particle size distribution (agglomeration state), morphology, and chemical composition of the four silica. It is well accepted that a proper physicochemical characterization of nanomaterials is achieved through a combination of techniques rather than an individual one [35–37]. The current most complete technique for studying NPs is TEM, since it provides particle size (in powder or dry state), morphology, and chemical composition (with and EDX detector) information; however, TEM is a low throughput technique because the measurement and analysis to achieve statistically relevant data of the three parameters is time-consuming.

To overcome this drawback, in this study, the SdFFF and DCS techniques were used to obtain, in a shorter time, information about the particle size distributions (PSDs), while the chemical surface and bulk analysis has been done by XPS and PIXE, respectively.

Characterization of the silica samples

The four synthetic amorphous silica samples consist of nano-sized primary particles, aggregated and agglomerated to build entities of larger sizes. When dispersed in water, the aggregates and the agglomerates break to smaller entities, whose sizes and relative amount depend on the dispersions method. The simplest procedure to disperse them in water consists of mixing the powders with a magnetic stirrer, for which the velocity of the stir bar and the time are important experimental parameters. Since the powders were dispersed in water without any treatment, the results of these investigations can be considered as relative to the first stage of the five advised by EFSA [10], i.e., "as manufactured."

Both SdFFF and DCS techniques are able to express the results of their separation analysis either in terms of relative weight % PSDs and relative number % PSDs, proving their compatibility with the EU definition of "nanomaterial" [11]. The conversion of the "weight" PSD in "number" PSD allows classifying immediately a sample as "nanomaterial" if the median of the distribution is ≤100 nm, but it must be underlined that when the detector is a conventional UV-vis detector or a laser, as in this work, the intensity of the light scattered by the particles (signal) is proportional to the sixth power of their diameter [14].

Figure 1 reports the relative number % PSDs of the four silica samples determined by DCS (graphs a and b) and SdFFF (graphs c and d). Both techniques classify all silica samples as "nanomaterial," even if the SdFFF S101 technical characteristics (rotor radius and maximum rotation speed) and of the low density of the particles (~2.2 g/mL) do not allow to resolve the particles/aggregates smaller than 30–40 nm. Consequently, the Aerosil particles smaller than 10 nm are visible only from the DCS graph (plot a), as the Tixosil particles of 20–30 nm from plot b.

Fig. 1

Particle size distributions (PSDs) of the A300, A380, T43, and T73 silica samples, dispersed by mechanical mixing: stirring time 15 min, velocity of the stir bar 400 rpm. (**a**, **c**) Relative number % PSDs achieved by DCS; (**b**, **d**) Relative number distributions determined by SdFFF

AQ5

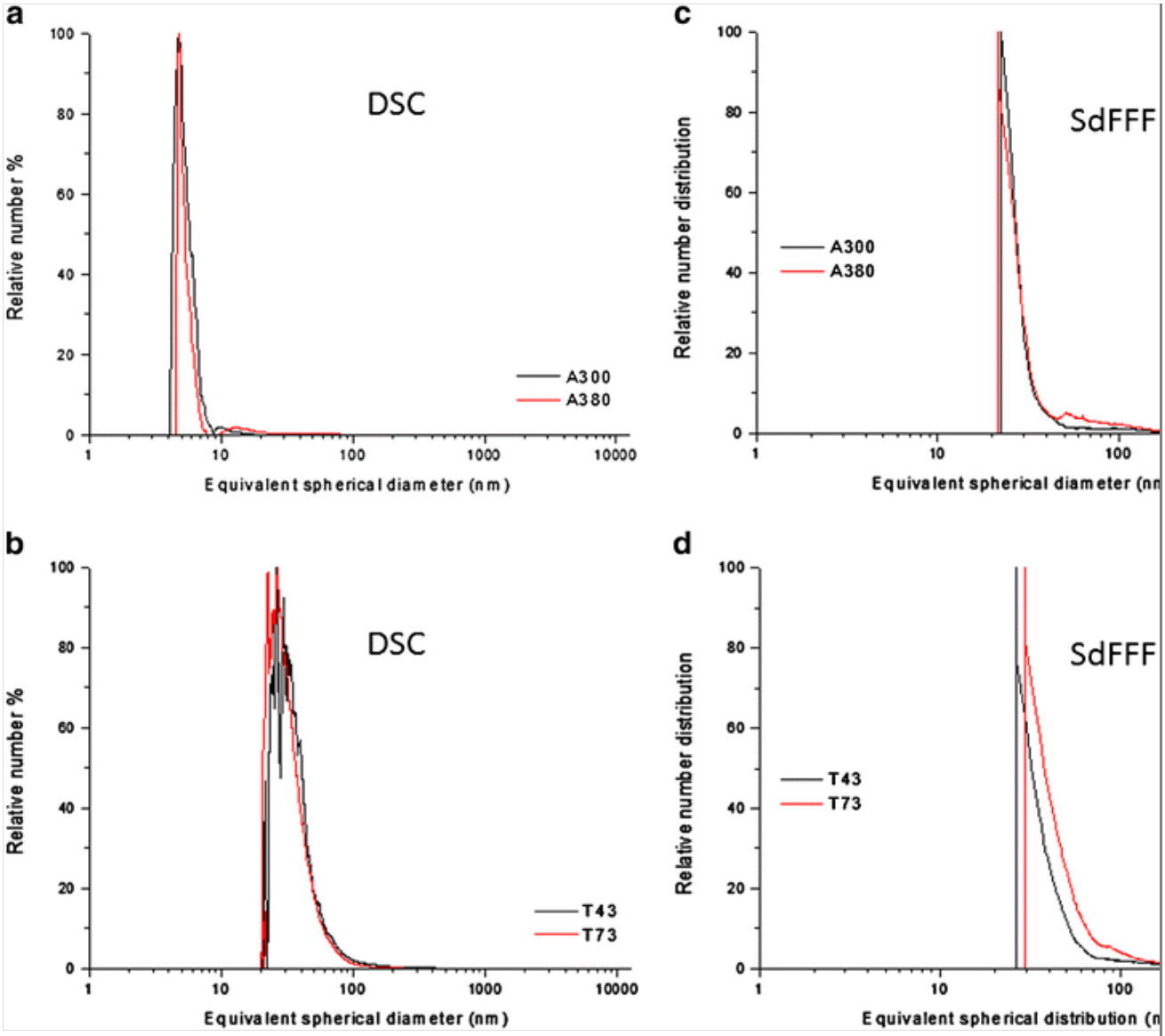

On the point of view of the EU definition, these are the required information; however, the relative number % PDSs sometimes do not allow to highlight details, which the relative mass % distributions do (Fig. 2). In this case, for example, the DCS weight distributions (Fig. 2a, height normalized) show clearly the 7-nm "primary" particle declared by the Aerosil producer [38], for both A300 and A380 samples, and the sizes displayed in Fig. 2b confirm that the T43 and T73 samples are suitable for cosmetics and personal care products [39].

Fig. 2

(**a**–**d**) A300, A380, T43, and T73 relative particle "mass" size distributions achieved by DCS and SdFFF, from which were derived the "number" distributions reported in Fig. 1

AQ6

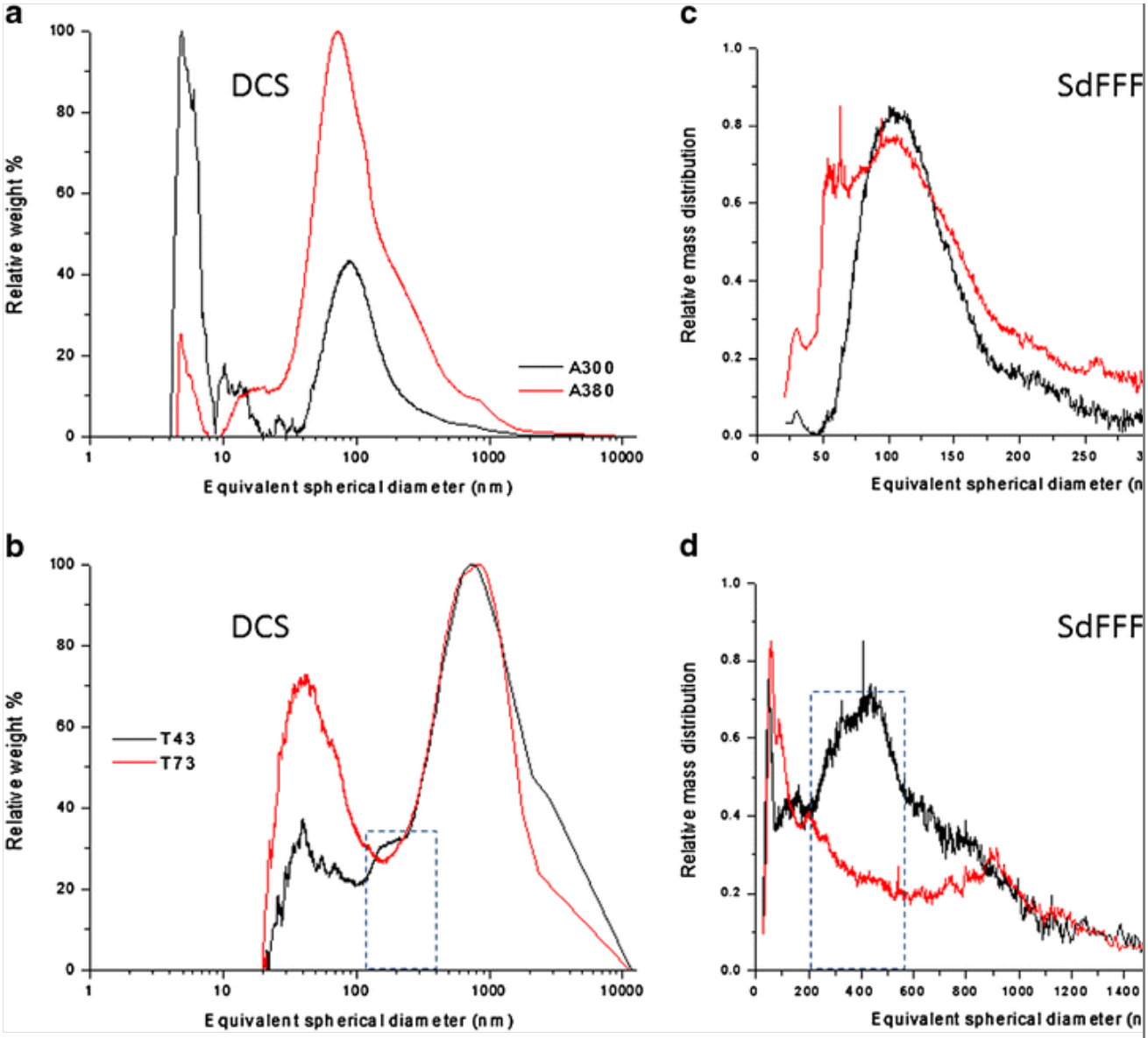

DCS and SdFFF complement very well in detecting the small particles and size ranges of different extension; for example, the SdFFF, opportunely set (size window 100–1400 nm), highlights the third population of 400 nm of the T43 sample (plot d), seen only as a small shoulder on the left of the second peak in Fig. 2b. Nevertheless, the certainty of dealing with single particles (<10 nm) or aggregates/agglomerates randomly broken can come only from SEM (or TEM) observations, as reported in Fig. 3.

Fig. 3

~~(a–d)~~ SEM pictures of the samples A300 (Mag 26 k), A380 (Mag 149 K), T43 (Mag 30 K), and T73 (Mag 50 k), respectively

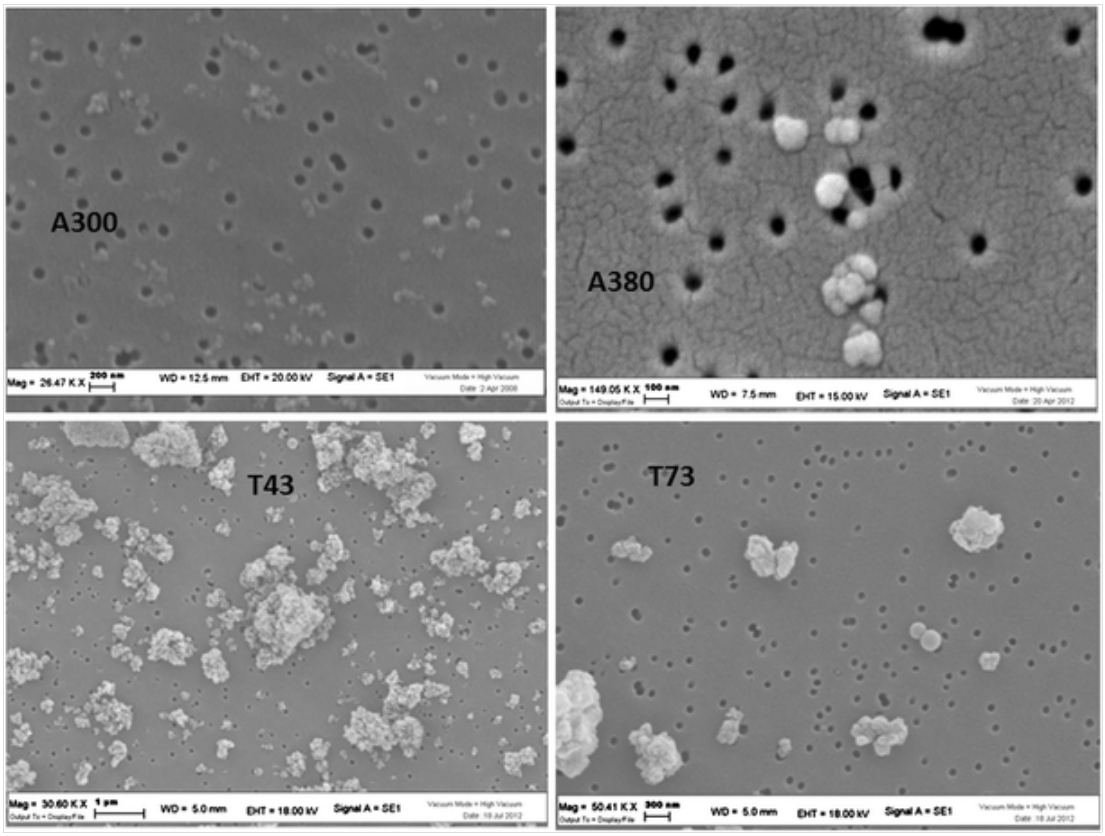

The size characterization of the silica samples was enriched by the surface and bulk chemical composition analyses, performed by XPS and PIXE, respectively. The XPS analyses, done on the powders “as received,” confirm Si and O as predominant elements in the surface top layer (5 nm deep), with an average O/Si ratio of 1.6 for the Aerosil samples and 1.7 for the Tixosil samples (see Table 1). The small amount of carbon, detected in all samples, is considered a surface contamination with this ubiquitous element, in line with the results achieved on similar samples, where the presence of carbon-oxygen compounds was hypothesized [40, 41].

The elemental chemical composition of a deeper surface layer (up to 40 μm) was determined by PIXE, but unlike the XPS analyses, only the T73 was analyzed as powder. Silicon was confirmed the most abundant element in all samples (~46.5 %—Table 2), followed by P (0.52 %—A300, 0.36 %—A380, 0.27 %—T43, 0.28 %—T73). The Aerosil samples resulted purer compared to the Tixosil samples, which both contained also S (0.28 %—T43 and 0.12 %—T73). The small amount of K, Ca, and Cl come most likely from the water used to disperse the samples, accumulated during the 10 depositions.

As a general conclusion, from these results, one might assert that the two Aerosil samples are very similar, as they are also the two Tixosil samples. The two type of silica differ in terms of impurities, in line with their suggested uses, but these different purity grades could imply a different surface reactivity during the formulation of products or with the physiological media if ingested.

Surface and bulk chemical composition of the A380 and T43 fractionated samples.

The protocol followed to disperse the particles in water (stirring or sonication) is an important experimental detail since the energy provided may modify the PSD and the surface composition of pristine particles. To deepen this aspect, the A380 and the T43 were selected to represent the two type of silica. A380 was preferred over A300 because of its higher surface area, while the sample T43 was preferred over T73 because recommended it is also for oral care formulations [42].

The silica suspensions were prepared by mixing the NPs with a magnetic stirrer (method A) and by using a US probe (method B). This "invasive" sonication method (direct contact of the suspension of the probe) was chosen instead of the water bath method in order to transfer to the NP suspension a very concentrated power through the tip [43].

The four suspensions (A380 son, A380 stirr, T43 son, and T43 stirr) were coarsely divided by centrifugation in two fractions, by setting theoretical size cutoffs of 40 nm (A380) and 300 nm (T43) (Fig. S1). The samples were very heterogeneous in sizes and their separation in fractions, performed in a single step, surely could not produce sharp cutoffs, but to improve the separation would have meant manipulating heavily the samples, with the risk of achieving a non-representative portion of the original silica. The sediment particles were re-dispersed in a few milliliters of deionized water, while the supernatant particles were concentrated by evaporating the exceeding water; at the end of the procedure, the sediment fractions resulted more concentrated than the supernatant fractions. The PSDs of the four fractions, controlled with both the DCS and SdFFF, are commented in the Supplementary Material and reported in Fig. S2 and S3.

The XPS data (Table 3) highlight an important increase in almost all cases of the relative amount of C, with respect to the original unfractionated samples (Table 1), likely because of the different procedures followed to prepare the specimens. The surface chemical composition data reported in Table 3 were determined on the particles dispersed in water, vigorously mixed (method A), or sonicated (method B), while the data of Table 1 refer to the silica powders. Method A surely favors the dissolution of the CO_2 in the suspension, causing an increase of the carbon-oxygen species (e.g., in the form of HCO_3^-), while method B removes the dissolved CO_2 from suspensions, leaving in the aqueous phase only the precipitated species ($CO_3^=$) or the organic contaminants. A closer analysis of the XPS C1s peak shape has revealed in fact the presence of at least two components, at 285 and 288.5 eV, ascribable to CC/CH and C=O bonds, respectively [40]. The highest amount of C was found in the sediment fractions (up to ~45.6 and 41.1 at.%) for the sample A380 and in the supernatant fractions for the sample T43.

The dispersion method affects also the surface Si content determined in the T43 fractions; in particular, both fractions achieved with the method A contain only the 14 % (5–6 at.%) of the Si average value (35 at.%). The synthesis method (precipitation) plays surely an important role in the T43 behavior in water. The mechanical action due to the stirring bar likely favors the surface dissolution, so that the Si atoms are released in the

solution and some Na atoms, entrapped in the solid structure as residual of the synthesis procedure become visible [44]. This dissolution process could be more efficient on the particles/aggregates with the smallest dimensions (supernatant) [45]. On the contrary, method B would seem let the surface chemical composition unaltered.

The data reported in Table 3 are surely not of simple interpretation, but it is quite clear that mechanical stirring, thought as the easiest dispersing method, induces the biggest compositional differences respect to the original analyses done on the powders.

To verify if the differences highlighted by XPS corresponds a structural difference, related with the particle/aggregate sizes, the fractions achieved with the method A were analyzed also by PIXE. The Si content was confirmed in both the sediment fractions (475,000 ppm, see Table 4 vs. Table 2), while the Si content of the supernatant fractions was significantly lower than initial concentrations, confirming the depletion observed by XPS. Sulfur was detected in both supernatant fractions, mainly in the T43 sample, where it was found also in the sediment, in line with the results achieved on the unfractionated powders. The mineral content observed in the supernatant fractions was ascribed to both the evaporation procedure ("blank" values were taken into account) and the ions enrichment due to the particle's washout, so that it might be concluded that ~~de facto~~*de facto*, there is not a substantial change from the bulk chemical composition.

Table 4

PIXE chemical composition of the fractions achieved from the samples A380 and T43, dispersed according the method A. Data corrected for the ionic content of the deionized water

	Si (ppm)	P (ppm)	S (ppm)	K (ppm)	Ca (ppm)	Cl (ppm)
A380 sediment	475,000 ± 3895					
A380 supernatant	116,732 ± 537	849 ± 118	20173 ± 139	1482 ± 38	1050 ± 34	10,101 ± 112
T43 sediment	475,000 ± 1853	3113 ± 640	5649 ± 282		260 ± 80	
T43 supernatant	5374 ± 138		71,064 ± 242	427 ± 25	1841 ± 38	3023 ± 87

Biological effects of commercial SiO_2 on human intestinal Caco-2 cells

In order to evaluate the biological effects of the different silica samples, human intestinal Caco-2 cells were incubated in the presence of 100 μg/mL of A300, A380, T43, or T73 NPs, dispersed by stirring (method A) and by sonication (method C).

The impact of these suspensions on cell viability was evaluated after 24 h of incubation by measuring the reduction of MTS tetrazolium salt into a colored formazan product and

by quantifying the amount of intracellular LDH released in cell culture medium (resulting from cell membrane damage) [46]. Non-viable cells or non-proliferative cells do not reduce MTS tetrazolium salt leading to a decrease of OD values.

Figure 4 shows that the T43 and T73 induced a slight decrease of MTS enzymatic reduction (Fig. 4a) and a slight increase of LDH release (Fig. 4b, c) suggesting a limited cytotoxic effect of these particles in comparison with positive control benzalkonium chloride (BC), leading to a drastic fall of cell viability. This result was independent on the applied dispersion method (stirring or sonication). After 24 h of incubation with either A300 or A380 (stirred or sonicated), a slight effect was observed with MTS assay (Fig. 4a) while no increase of LDH release was measured in comparison with non-treated cells (CTL, Fig. 4c), suggesting that A300 and A380 could slightly impact on cell proliferation without inducing cell damage.

Fig. 4

Evaluation of the cytotoxic effects of T43, T73, A430, and A300 NPs on Caco-2 cells measured through the MTS and LDH assays. Cells were incubated 24 h in the presence or not (control, CTL) of 100 μg/ml of stirred or sonicated SiO_2 NPs. (**a**) Effect of T43, T73, A430, and A300 NPs on MTS enzymatic reduction. The results are expressed as means ± SD ($n = 3$), normalized to control, and presented as percentages of control. *$P < 0.05$ vs. control; **$P < 0.01$ vs. control; ***$P < 0.001$. Benzalkonium chloride (BC; 0.01 mg/mL) was used as positive control. (**b**, **c**) Effect of T43, T73, A430, and A300 NPs on LDH release. (**c**) is the enlargement of (**b**). The results are expressed as means ± SD ($n = 3$) and normalized to control. *$P < 0.05$ vs. control; **$P < 0.01$ vs. control. BC (0.01 mg/mL) was used as positive control

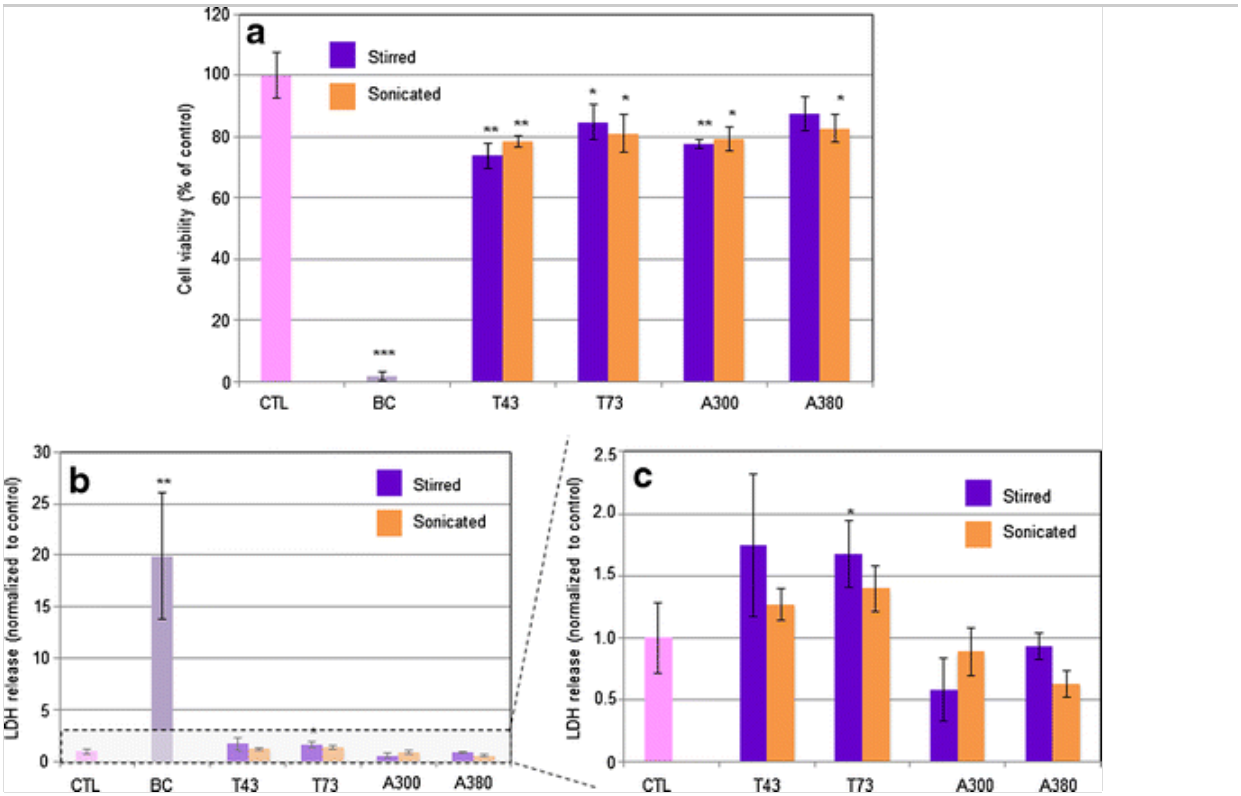

Potential pro-apoptotic effect of SiO_2 NPs was evaluated by measuring the activity of caspases 3/7 (Fig. 5). Caspases belong to the cysteine aspartic acid-specific protease family and play key roles in apoptosis in mammalian cells [47, 48]. Upon apoptosis induction, activated caspases participate in a cascade of cleavage events leading to the disabling of key homeostatic and repair enzymes and finally to cell death.

Fig. 5

Evaluation of the pro-apoptotic effect of T43, T73, A430, and A300 NPs. Caco-2 cells were incubated 24 h in the presence or not (control, CTL) of 100 μg/ml of stirred or sonicated SiO_2 NPs. Pro-apoptotic effect of silica NPs was evaluated by measuring the activity of caspases 3 and 7. The results are expressed as means ± SD ($n = 3$) and normalized to control. *$P < 0.05$ vs. control; ***$P < 0.001$ vs. control. Butyrate (50 mM) was used as positive control

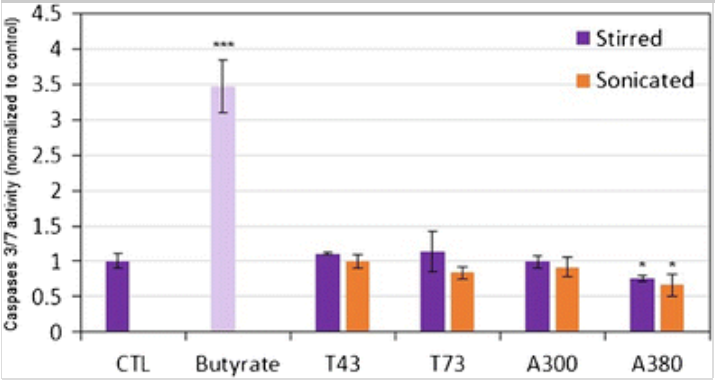

No activation of effector caspases 3 and 7 was observed in Caco-2 cells after 24 h of incubation, suggesting that silica NPs do not have pro-apoptotic effects (Fig. 5).

Pro-inflammatory effect of these silica samples was evaluated in parallel by measuring the amount of IL-8 released in cell culture medium after 24 h of incubation. IL-1β was used as a positive control. No IL-8 was detected in the cell culture medium after 24 h of incubation with 100 μg/mL of either T43, T73, A380, or A300 (data not shown—protocol of the experiments is reported in the Supplementary Material §3S).

Biological effects of the fractionated SiO_2 on human intestinal Caco-2 cells

In order to verify whether potential toxic effects could be related with the particle sizes and the sonication treatment, the MTS viability assay was performed also on the fractionated A380 and T43 samples dispersed by stirring and with the US probe (Fig. 6). The probe sonication was a substitute to the water bath sonication to stress the experimental conditions after having observed limited cytotoxic effects on all whole samples, independently of the dispersion method.

Fig. 6

MTS assay on T43 and A380 supernatant and sediment fractions. Caco-2 cells were

incubated 24 h in the presence or not (control, CTL) of 100 μg/ml of T43 and A380 supernatant and sediment fractions. The results of the MTS enzymatic reduction are expressed as means ± SD ($n = 3$) and presented as percentages of control. *$P < 0.05$ vs. control; **$P < 0.01$ vs. control; ***$P < 0.001$ vs. control; $^{\#}P < 0.05$ vs. supernatant fraction; $^{\#\#}P < 0.01$ vs. supernatant fraction. Benzalkonium chloride (BC, 0.01 mg/mL) was used as positive control

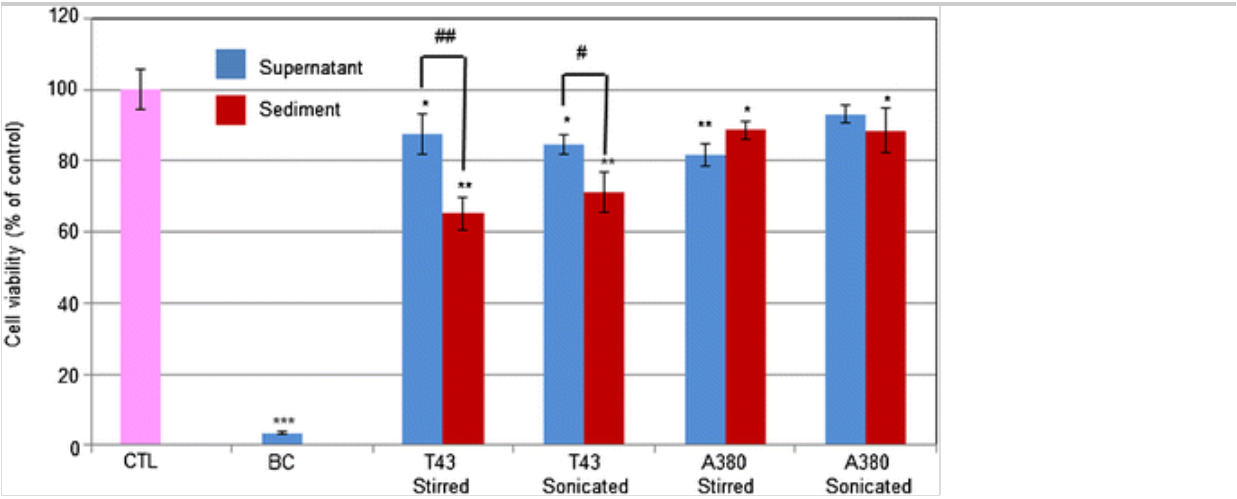

All supernatant fractions (corresponding to particles <40 and 300 nm, respectively), independently of the dispersion method, induced a slight decrease of MTS enzymatic reduction. Between A380 sediment and supernatant fractions, no difference was noted, while a significant more important and interesting effect was observed after incubation with T43 sediment fraction. Since the surface chemical composition of these particles is similar to the whole sample (Table 3), the biological effect could be related to the T43 agglomerate sizes. These results might appear surprising since other studies have shown that silica particles with average sizes larger than 100 nm or agglomerated (independently of the primary particle size) used at the same concentration level of this study (100 μg/mL) have a limited toxicological impact and toxic effects were obtained only after cell exposure to high concentrations (1 to 10 mg/mL) [49].

The whole set of data suggests that SiO_2 NPs have only a limited toxic effect on Caco-2 cells confirming previous studies describing a limited toxic effect of silica [18, 50]. For instance, Van der Zande et al. showed that oral exposure of rats to silica did not result in a clear tissue accumulation of silica nor increase toxic biochemical and immunological markers in blood and isolated cells after 28 days of exposure [20]. Some liver fibrolysis was only observed after 84 days of exposure to high amount of silica not really representative of the current exposure of consumers.

Incubation of the silica A380 and T43 samples in simulated gastric fluid

In order to mimic a stomach digestion, the A380 and T43 dried sediment fractions (100 μg/mL), dispersed by stirring or sonicated with the probe (Table S2), were incubated for 4 h in a simulated gastric fluid, knowing that exposure to low pH affected

the cytotoxicity of some NPs, like for instance, CdSe quantum dots [51].

The incubation in acidic environment determined a MTS enzymatic reduction (toxic effect) (Fig. 7) similar to the slight decrease observed in Fig. 4a, when the whole samples were stirred or bath sonicated, and as observed in Fig. 6, where the sediment and the supernatant fractions (stirred or probe sonicated) were compared. Acidic treatment would seem to reduce only the impact of T43 sediment fraction obtained by stirring, but the high standard deviation limits the result reliability.

Fig. 7

Evaluation of the effect of acidic treatment (simulated digestion) on the silica toxicity. T43 and A380 sediment fractions or powder were incubated 4 h in gastric like fluid and incubated 24 h on Caco-2 cells at 100 µg/ml. Cytotoxicity was assayed by MTS enzymatic reduction. The results are expressed as means ± SD ($n = 3$) and presented as percentages of control. $^{**}P < 0.01$ vs. control; $^{***}P < 0.001$ vs. control. Benzalkonium chloride (BC; 0.01 mg/mL) was used as positive control

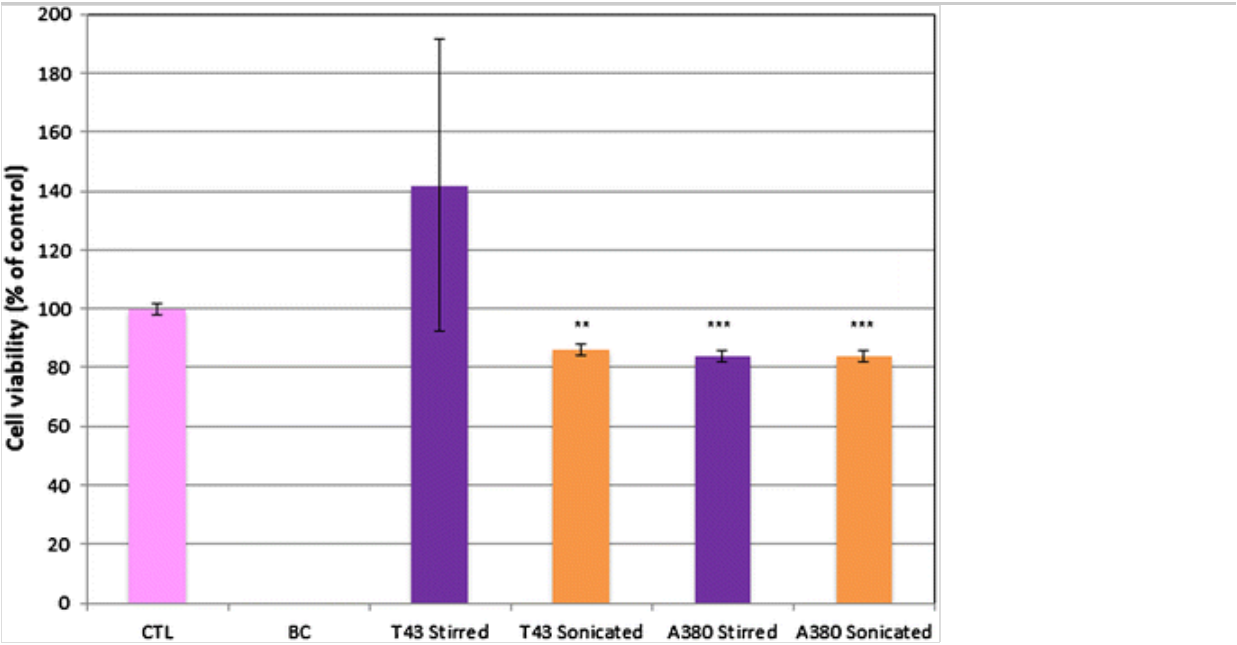

These data are in accordance with other in vitro studies that have shown that silica NP pre-treatment under simulated gastric and intestinal conditions did not modify their cytotoxic effect or IL-8 secretion from Caco-2 cells [52]. These authors also showed different biological impact depending on the differentiation status of Caco-2 cells: undifferentiated Caco-2 cells being more sensible to silica toxic effects than differentiated Caco-2 cells [53].

The limited toxicological impact of silica samples used at high concentration on undifferentiated Caco-2 cells confirm the limited toxic effect of these T43, T73, A300, and A380 silica samples. As far as the impact of dispersion method on biological effect of SiO_2 NPs is concern, no difference in biological effects was observed between sonicated or non-sonicated SiO_2 particles. This result agrees with recent publications,

which have shown that either sonicated or stirred copper oxide (CuO) NPs could induced similar toxic effects on different skin cell lines, even if NP surface chemical composition and size distribution were modified by sonication [54]. These authors suggested that these similar biological effects could be due to a similar coating of NPs by proteins and molecules present in cell culture medium independently of the NP agglomeration state or surface modifications exposing cells to similar protein corona-NP complexes [53, 54]. On the other hand, other studies have shown that sonication could potentially modify the toxic effects of NPs; for example, sonicated multi-walled carbon nanotubes (MWCNTs) drastically decrease N-hTERT keratinocytes viability in comparison with stirred MWCNT [55], and sonicated copper (Cu) NPs increase the A549 cells mortality [53]. In those cases, the modification of NP dispersion state (agglomeration, aggregation, etc.) and/or alteration of the structure and surface of NPs [16] were indicated as important parameters to explain modified biological effects of NPs after sonication.

Consumer products

With the aim of pointing out pros and cons of this approach to the analysis of commercial products, a barley coffee and a “Cappuccino mix” were prepared as suggested on the label for consumers. The relative weight distributions achieved by DCS prove that the cappuccino mix contains particles and/or aggregates of sizes spanning between 30 nm up to 2 μm, while the particles detected in the barley coffee have mainly dimensions lower than 10 nm and only a limited amount of them have sizes between 100 nm and 1 μm (Fig. 8a). These data well complement with previous results achieved by SdFFF [38]. These DCS data highlight the lightest particles, <10 nm, that SdFFF was unable to separate from the void time [38] and that could be SiO_2 or others insoluble particulate components. The DCS relative number distributions (Fig. 8b) asses that both commercial products contain “nanoparticles” with the important consideration that the barley coffee should contain only roasted starch grains, while the “Cappuccino mix” contains E551.

Fig. 8

DCS relative weight % (**a**) and relative particle “number” (**b**) size distribution of the “Cappuccino mix” (contained E551) and of the instant barley coffee (silica free) dissolved in hot deionized water. The drink suspensions were prepared following the label indication for a homemade preparation, i.e., they were prepared and analyzed as a consumer would ingest them

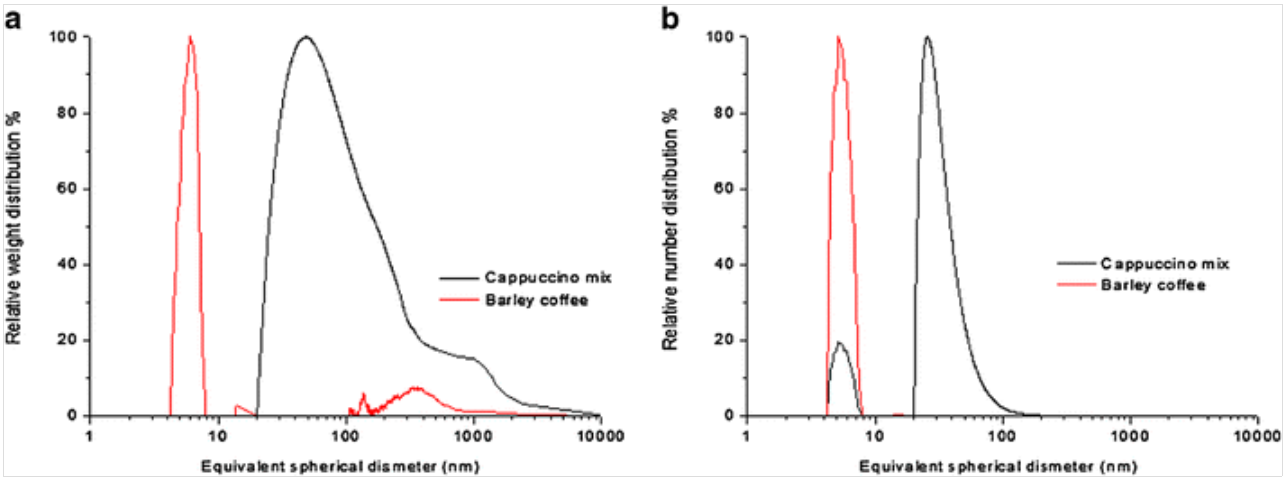

The first remark for applying this experimental approach to an unknown commercial sample is to add, on- or offline, a multi-element-specific detector, such as ICP-MS, ICP-AES, or GFAAS [56–58] to the FFF instrument, to establish the nature of the NPs (isolated from the matrix) and fractionated by mass. Unfortunately, DCS does not allow such a specific detection because it is not a flow-separation instrument, but this reinforces its complementarity with the SdFFF.

The PIXE chemical analysis confirmed the absence of Si in the instant barley coffee, also as native element, which is understandable since silica is present in the outer walls of the husk [59, 60], which is not affected during malting (Table 5). The ability of PIXE to quantify elements in complex matrices is used to determine the amount of Si in the cappuccino mix: the ~370 ppm correspond to 0.0783 ± 0.0169 % *w*/*w* of SiO_2, a value in agreement with the 0.0666 ± 0.0055 % *w*/*w* reported in [38], well below than the 1 % *w*/*w*, the limit allowed for the E551 as food additive [61].

Table 5

Chemical composition determined by PIXE of the consumer products

Sample	Si (ppm)	P (ppm)	S (ppm)	Cl (ppm)	K (ppm)	Ca (ppm)	Ti (ppm)
Cappuccino	366 ± 79	3550 ± 74	859 ± 37	2229 ± 45	8828 ± 72	2129 ± 53	116 ± 18
Instant barley coffee		1970 ± 58	382 ± 28	827 ± 31	3709 ± 45	161 ± 24	147 ± 19

The second remark concerns the biological effects of the silica particles contained in the “Cappuccino mix” on human intestinal Caco-2 cells, which were not evaluated because of the extremely low concentration of SiO_2 in the commercial powder. Preparation of a 1-mg SiO_2/mL suspension by extracting the particles from the powder would have meant to treat an amount of product suitable to make liters of cappuccino drink, a dose far from a reasonable daily use. On the other hand, also considering for a possible accumulation effect related to a regular assumption of this drink, the extraction

procedure from the powder could have determined, for example, particle aggregation or surface chemistry modifications such to lose the representativeness of the final portion.

Conclusions

The analytical techniques for the particle size distribution and the chemical composition determination described in this study are relevant to characterize nanomaterials, according to the EC recommendations.

The four silica samples, currently used in food or consumer products, could be classified as “nanomaterials” (under the EC Recommendation) following analysis by DCS and SdFFF. The XPS and PIXE chemical analyses confirmed that Si is the prevalent element in all samples; the two Aerosil being purer than the Tixosil samples, in line with their proposed uses.

The dispersion procedure is very important since it defines the particle size distribution of the dispersed particles and it might affect the particle surface chemical composition. Unexpectedly, the mechanical mixing has determined a significant variation of the chemical composition of the outer particle shell, evidenced by the XPS measurements, while the ultrasound treatment is confirmed as a very efficient method to destroy aggregates, as highlighted by DCS and SdFFF analyses.

The potential toxic effects of the SiO_2 samples, used at high concentration (100 μg/mL), were investigated on undifferentiated human intestinal Caco-2 cells. Viability assays showed a slight toxic effect of all particles, independently of the dispersion method, suggesting the relative innocuity of these silica samples.

Finally, two commercial food products, a “Cappuccino mix” and an instant barley coffee, dispersed in water as suggested on their labels in terms of stirring and concentration, contained NPs when analyzed by DCS. Barley coffee did not contain silica particles, while the “Cappuccino mix” contained the E551 additive in a concentration well below the limit indicated by law (1 % *w*/*w*), limiting the possible concern among consumers, in the light also of their insignificant biological effects here verified.

Acknowledgments

This research received support from the QualityNano Project http://www.QualityNano.eu which is financed by the European Community Research Infrastructures under the F7 Capacities Programme (grant no. INFRA-2010-262163) and its partner University of Namur.
This work was also founded by the University of Ferrara (Fondo di Ateneo per la Ricerca Scientifica FAR 2013).

Compliance with ethical standards

Conflict of interest The authors declare that they have no competing interests.

Electronic supplementary material

Below is the link to the electronic supplementary material.

ESM 1

(PDF 434 kb)

References

AQ7

1. Napierska D, Thomassen LCJ, Lison D, Martens AJ, Hoet PH (2010) The nanosilica hazard: another variable entity. Part Fibre Toxicol 7(1):1–39

2. Cushen M, Kerry J, Morris M, Cruz-Romero M, Cummins E (2012) Nanotechnologies in the food industry—recent developments, risks and regulation. Trends Food SciTech 24:30–46

3. Peters R, Kramer E, Oomen AG, Rivera ZE, Oegema G, Tromp PC, Fokkink R, Rietveld A, Marvin HJ, Weigel S, Peijnenburg AA, Bouwmeester H (2012) Presence of nano-sized silica during in vitro digestion of foods containing silica as a food additive. ACS Nano 6(3):2441–2451

4. Rashidi L, Khosravi-Darani K (2011) The applications of nanotechnology in food industry. Crit Rev Food Sci Nutr 51(8):723–730

5. Art 18 (3), EU's 2011 Regulation on Food Information to Consumers (1169/2011)

6. Regulation (EC) No 1223/2009 of the European Parliament and of the Council of 30 November 2009 on cosmetic products

7. Nanoparticles in Food: close, but not too close. Nano the magazine for small science.http://nanomagazine.co.uk Accessed 30 March 2015

8. Online document Nanotechnologies http://ec.europa.eu/health/opinions2 /en/nanotechnologies/l-2/6-health-effects-nanoparticles.htm Accessed 30 March 2015

9. Dhawan A, Sharma V (2010) Toxicity assessment of nanomaterials: methods and challenges. Anal Bioanal Chem 398:589–605

10. REF EFSA Journal (2011);9(5):2140 36 pp doi: 10.2903/j.efsa.2011.2140

11. Commission Recommendation of 18 October 2011 on the definition of nanomaterial (2011) (2011/696/EU) 275: 38–40

12. Schimpf ME, Caldwell KD, Giddings JC (2000) Field-flow fractionation handbook. Wiley-Interscience, New York

13. Merkus HG (2009) Particle size measurements—fundamentals, practice, quality. Particle technology series, vol 17. Springer Netherlands, Netherlands, ~~pp~~ pp 329–~~pp~~ 334

14. Bohren CF, Huffman DR (1983) Absorption and scattering of light by small particles. John Wiley & Sons, New York

15. Lozano O, Laloy J, Alpan L, Mejia J, Rolin S, Toussaint O, Dogné JM, Lucas S, Masereel B (2012) Effects of SiC nanoparticles orally administered in a rat model: biodistribution, toxicity and elemental composition changes in feces and organs. Toxicol Appl Pharmacol 264:232–245

16. Mejia J, Tichelaar F, Saout C, Toussaint O, Bernard M, Mekhalif Z, Lucas S, Delhalle J (2011) Effects of the dispersion methods in Pluronic F108 on the size and the surface composition of MWCNTs and their implications in toxicology assessment. J Nanopart Res 13(2):655–667

17. Mejia J, Valembois V, Piret J-P, Tichelaar F, Bernard M, Toussaint O, Delhalle J, Mekhalif Z, Lucas S (2012) Are stirring and sonication pre-dispersion methods equivalent for the in vitro toxicology evaluation of SiC and TiC? J Nanopart Res 14(4):815–833

18. Yang Y-X, Song Z-M, Cheng B, Xiang K, Chen X-X, Liu J-H, Cao A, Wang Y, Liu Y, Wang H (2014) Evaluation of the toxicity of food additive silica nanoparticles on gastrointestinal cells. J Appl Toxicol 34(4):424–435

19. Elsaesser A, Vyvyan Howard C (2012) Toxicology of nanoparticles. Adv Drug Deliv Rev 64(2):129–137

20. van der Zande M, Vandebriel RJ, Groot MJ, Kramer E, Herrera Rivera ZE, Rasmussen K, Ossenkoppele JS, Tromp P, Gremmer ER, Peters RJB, Hendriksen PJ, Marvin HJP, Hoogenboom RLAP, Peijnenburg AACM, Bouwmeester H (2014) Sub-chronic toxicity study in rats orally exposed to nanostructured silica. Part Fibre Toxicol 11:8–27

21. van Kesteren PCE, Cubadda F, Bouwmeester H, van Eijkeren JCH, Dekkers S, de Jong WH, Oomen AG (2015) Novel insights into the risk assessment of the nanomaterial synthetic amorphous silica, additive E551, in food. Nanotoxicology 18:1–10

22. Schrurs F, Lison D (2012) Focusing the research efforts. Nat Nanotechnol

7:546–548

23. Shang L, Nienhaus K, Nienhaus GU (2014) Engineered nanoparticles interacting with cells: size matters. J Nanobiotechnology 12:5–26

24. Bhowmick TK, Yoon D, Patel M, Fisher J, Ehrman S (2010) In vitro effects of cisplatin-functionalized silica nanoparticles on chondrocytes. J Nanopart Res 12:2757–2770

25. Dekkers S, Bouwmeester H, Bos PMJ, Peters RJB, Rietveld AG, Oomen AG (2013) Knowledge gaps in risk assessment of nanosilica in food: evaluation of the dissolution and toxicity of different forms of silica. Nanotoxicology 7(4):367–377

26. Pedrazzi V, Del Ciampo JO, do Nascimento C, Mardegan Issa JP (2009) Evaluation of some biological aspects of the presence of abrasive silica and thickening silica in basic formulations of dentifrices. Int J Morphol 27(1):159–168

27. Laoutid F, Ferry L, Leroy E, Lopez Cuesta JM (2006) Intumescent mineral fire retardant systems in ethylene–vinyl acetate copolymer: effect of silica particles on char cohesion. Polym Degrad Stabil 91:2140–2145

28. Cascio C, Gilliland D, Rossi F, Calzolai L, Contado C (2014) Critical experimental evaluation of key methods to detect, size and quantify nanoparticulate silver. Anal Chem 86:12143–12151

29. Williams PS, Giddings JC (1994) Theory of field-programmed field-flow fractionation with corrections for steric effects. Anal Chem 66:4215–4228

30. Lozano O, Mejia J, Piret J-P, Saout C, Dogné J-M, Toussaint O, Lucas S (2013) How does the deposited dose of oxide nanomaterials evolve in an in vitro assay? J Phys: Conf Ser 429:012013

31. IAEA (1989) International Atomic Energy Agency. Reference materials catalogue and documents. Available from the website: http://nucleus.iaea.org /rpst/referenceproducts/ReferenceMaterials/Trace_Elements_Methylmercury/IAEA-153.htm Accessed 30 March 2015

32. IAEA (1990) International Atomic Energy Agency. Reference materials catalogue and documents. Available from the website: http://nucleus.iaea.org /rpst/referenceproducts/ReferenceMaterials/Trace_Elements_Methylmercury/IAEA-155.htm Accessed 30 March 2015

33. Lozano O, Toussaint O, Dogné J-M, Lucas S (2010) The use of PIXE for engineered nanomaterials quantification in complex matrices. J Phys: Conf Ser 429:012010

34. Ruemmele FM, Dionne S, Qureshi I, Sarma DSR, Levy E, Seidman EG (1999) Butyrate mediates Caco-2 cell apoptosis via up-regulation of pro-apoptotic BAK and inducing caspase-3 mediated cleavage of poly-(ADP-ribose) polymerase (PARP). Cell Death Differ 6:729–735

35. Bouwmeester H, Lynch I, Marvin HJP, Dawson KA, Bergers M, Braguer D, Byrne HJ, Casey A, Chambers G, Clift MJ, Elia G, Fernandes TF, Fjellsbø LB, Hatto P, Juillerat L, Klein C, Kreyling WG, Nickel C, Riediker M, Stone V (2011) Minimal analytical characterization of engineered nanomaterials needed for hazard assessment in biological matrices. Nanotoxicology 5(1):1–11

36. Lisinger TPJ, Roebben G, Gilliland D, Calzolai L, Rossi F, Gibson N,Klein C (2012) Requirements on measurements for the implementation of the European Commission definition of the term 'nanomaterial'. European Commission, Joint Research Centre

37. Roebben G, Rauscher H, Amenta V, Aschberger K, Sanfeliu AB, Calzolai L, Emons H, Gaillard C, Gibson N, Holzwarth U et al (2014) Towards a review of the EC Recommendation for a definition of the term "nanomaterial" Part 2: Assessment of collected information concerning the experience with the definition. European Commission, Joint Research Centre

38. Contado C, Ravani L, Passarella M (2013) Size characterization by sedimentation field flow fractionation of silica particles used as food additives. Anal Chim Acta 788:183–192

39. http://www.rhodia.com/en/markets_and_products/product_finder /product_details.tcm?productCode=90004254&productName=Tixosil%C2%AE+73 Accessed Sept 2014

40. Rasmussen K, Mech A, Mast J, De Temmerman P-J, Waegeneers N, Van Steen F, Pizzolon J.C., De Temmerman L, Van Doren E, Jensen K.A., Birkedal R, Levin M, Nielsen SH, Koponen IK, Clausen PA, Kembouche Y, Thieriet N, Spalla O, Giuot C, Rousset D, Witschger O, Bau S, Bianchi B, Shivachev B, Gilliland D, Pianella F, Ceccone G, Cotogno G, Rauscher H, Gibson N, Stamm H (2013) Synthetic amorphous silicon dioxide (NM-200, NM-201, NM-202, NM-203, NM-204): characterisation and physico-chemical properties. JRC Repository: NM-series of Representative Manufactured Nanomaterials

41. Baer DR, Gaspar DJ, Nachimuthu P, Techane S, Castner D (2010) Application of surface chemical analysis tools for characterization of nanoparticles. Anal Bioanal Chem 396(3):983–1002

42. http://www.rhodia.com.br/en/markets_and_products/product_finder

/product_details.tcm?productCode=90004252&productName=Tixosil%C2%AE+43 Accessed Jan 2015

43. JS. Taurozzi, VA. Hackley, MR (2012) Wiesner preparation of nanoparticle dispersions from powdered material using ultrasonic disruption version 1.1http://dx.doi.org/ 10.6028/NIST.SP.1200-2 or http://nvlpubs.nist.gov/nistpubs /SpecialPublications/NIST.SP.1200-2.pdf (Last accessed June 2015)

44. Mi Lim H, Lee J, Jeong J-H, Oh S-G, Lee S-H (2010) Comparative study of various preparation methods of colloidal silica. Engineering 2:998–1005

45. Synthetic Amorphous Silica. JACC No.51 Brussels (2006) http://members.ecetoc.org/Documents/Document/JACC%20051.pdf Accessed March 2015

46. Han X, Gelein R, Corson N, Wade-Mercer P, Jiang J, Biswas P, Finkelstein JN, Elder A, Oberdörster G (2011) Validation of an LDH assay for assessing nanoparticle toxicity. Toxicology 287(1–3):99–104

47. Nicholson DW, Ali A, Thornberry NA, Vaillancourt JP, Ding CK, Gallant M, Gareau Y, Griffin PR, Labelle M, Lazebnik YA, Munday NA, Raju SM, Smulson ME, Yamin TT, Yu VL, Mille DK (1995) Identification and inhibition of the ICE/CED-3 protease necessary for mammalian apoptosis. Nature 376:37–43

48. Nicholson DW, Thornberry NA (1997) Caspases: Killer proteases. TIBS 22:299–306

49. Sakai-Kato K, Hidaka M, Un K, Kawanishi T, Okuda H (2014) Physicochemical properties and in vitro intestinal permeability properties and intestinal cell toxicity of silica particles, performed in simulated gastrointestinal fluids. Biochim Biophys Acta 1840:1171–1180

50. Sergent JA, Paget V, Chevillard S (2012) Toxicity and genotoxicity of nano-SiO_2 on human epithelial intestinal HT-29 cell line. Ann Occup Hyg 56(5):622–630

51. Wang L, Nagesha DK, Selvarasah S, Dokmeci MR, Carrier RL (2008) Toxicity of CdSe nanoparticles in Caco-2 cell cultures. J Nanobiotechnology 6:11–26

52. Gerloff K, Pereira DIA, Faria N, Boots AW, Kolling J, Förster I, Albrecht C, Powell JJ, Schins RPF (2013) Influence of simulated gastro-intestinal conditions on particle-induced cytotoxicity and interleukin-8 regulation in differentiated and undifferentiated Caco-2 cells. Nanotoxicology 7:353–366

53. Cronholm P, Midander K, Karlsson HL, Elihn K, Wallinder IO, Moller L (2011) Effect of sonication and serum proteins on copper release from copper nanoparticles

and the toxicity towards lung epithelial cells. Nanotoxicology 5(2):269–281

54. Piret JP, Mejia J, Lucas S, Zouboulis CC, Saout C, Toussaint O (2014) Sonicated and stirred copper oxide nanoparticles induce similar toxicity and pro-inflammatory responses in N-hTERT keratinocytes and SZ95 sebocytes. J Nanop Res 16:2337

55. Vankoningsloo S, Piret JP, Saout C, Noel F, Mejia J, Zouboulis CC, Delhalle J, Lucas S, Toussaint O (2010) Cytotoxicity of multi-walled carbon nanotubes in three skin cellular models: effects of sonication, dispersive agents and corneous layer of reconstructed epidermis. Nanotoxicology 4(1):84–97

56. López-Heras I, Madrid Y, Cámara C (2014) Prospects and difficulties in TiO_2 nanoparticles analysis in cosmetic and food products using asymmetrical flow field-flow fractionation hyphenated to inductively coupled plasma mass spectrometry. Talanta 124:71–78

57. Contado C, Pagnoni A (2008) TiO_2 in commercial sunscreen lotion: flow field-flow fractionation and ICP-AES together for size analysis. Anal Chem 80:7594–7608

58. Contado C, Pagnoni A (2012) A new strategy for pressed powder eye shadow analysis: allergenic metal ion content and particle size distribution. Sci Total Environ 432:173–179

59. NIIR Board of Consultants & Engineer (2006) Wheat, rice, corn, oat, barley and sorghum processing handbook (Cereal Food Technology) NATIONAL INSTITUTE OF INDUSTRIAL RESEARCH

60. Gupta M, Abu-Ghannam N, Gallaghar E (2010) Barley for brewing: characteristic changes during malting, brewing and applications of its by-products. Compr Rev Food Sci F 9(3):318–328

61. EUROPEAN PARLIAMENT AND COUNCIL DIRECTIVE N° 95/2/EC of 20 February 1995 on food additives other than colours and sweeteners. Gazzetta ufficiale n. L 61 del 18.3.1995. http://ec.europa.eu/food/fs/sfp/addit_flavor /flav11_en.pdf Accessed March 2015